The Omp85-Related Chloroplast Outer Envelope Protein OEP80 Is Essential for Viability in Arabidopsis[1][W][OA]

Ramesh Patel, Shih-Chi Hsu, Jocelyn Bédard, Kentaro Inoue, and Paul Jarvis*

Department of Biology, University of Leicester, Leicester LE1 7RH, United Kingdom (R.P., J.B., P.J.); and Department of Plant Sciences, University of California, Davis, California 95616 (S.-C.H., K.I.)

β-Barrel proteins of the Omp85 (Outer membrane protein, 85 kD) superfamily exist in the outer membranes of Gram-negative bacteria, mitochondria, and chloroplasts. Prominent Omp85 proteins in bacteria and mitochondria mediate biogenesis of other β-barrel proteins and are indispensable for viability. In Arabidopsis (*Arabidopsis thaliana*) chloroplasts, there are two distinct types of Omp85-related protein: Toc75 (Translocon at the outer envelope membrane of chloroplasts, 75 kD) and OEP80 (Outer Envelope Protein, 80 kD). Toc75 functions as a preprotein translocation channel during chloroplast import, but the role of OEP80 remains elusive. We characterized three T-DNA mutants of the Arabidopsis OEP80 (AtOEP80) gene. Selectable markers associated with the *oep80-1* and *oep80-2* insertions segregated abnormally, suggesting embryo lethality of the homozygous genotypes. Indeed, no homozygotes were identified among >100 individuals, and heterozygotes of both mutants produced approximately 25% aborted seeds upon self-pollination. Embryo arrest occurred at a relatively late stage (globular embryo proper) as revealed by analysis using Nomarski optics microscopy. This is substantially later than arrest caused by loss of the principal Toc75 isoform, atToc75-III (two-cell stage), suggesting a more specialized role for AtOEP80. Surprisingly, the *oep80-3* T-DNA (located in exon 1 between the first and second ATG codons of the open reading frame) did not cause any detectable developmental defects or affect the size of the AtOEP80 protein in chloroplasts. This indicates that the N-terminal region of AtOEP80 is not essential for the targeting, biogenesis, or functionality of the protein, in contrast with atToc75-III, which requires a bipartite targeting sequence.

Chloroplasts and mitochondria evolved from bacteria through endosymbiosis. Recently, a family of β-barrel proteins related to Omp85 (Outer membrane protein, 85 kD) from *Neisseria meningitidis* was found in the outer membranes of Gram-negative bacteria, mitochondria, and chloroplasts (Yen et al., 2002; Gentle et al., 2005). Some bacteria contain multiple Omp85-related proteins, with the different homologs playing distinct roles in protein secretion (Jacob-Dubuisson et al., 2004) or the sorting of β-barrel proteins to the outer membrane (Voulhoux et al., 2003; Wu et al., 2005). By contrast, there appears to be just a single functional Omp85 homolog in mitochondria (Sam50 [Sorting and assembly machinery, 50 kD]; alterna-tively, Tob55 [Topogenesis of β-barrel proteins, 55 kD]), and this mediates β-barrel insertion into the membrane (Kozjak et al., 2003; Paschen et al., 2003; Gentle et al., 2004), as well as the insertion of other outer membrane proteins (Stojanovski et al., 2007).

Unlike mitochondria, chloroplasts contain at least two distinct types of Omp85 homolog, namely, Toc75 (Translocon at the outer envelope membrane of chloroplasts, 75 kD) and OEP80 (Outer Envelope Protein, 80 kD). Because homologs exist in extant cyanobacteria (one of which was shown to be essential for viability), these proteins are postulated to be derived from a common ancestor in the original endosymbiont (Bölter et al., 1998; Reumann et al., 1999, 2005). Detailed phylogenetic analyses suggested that Toc75 and OEP80 diverged early in the evolution of chloroplasts (Inoue and Potter, 2004).

Pea (*Pisum sativum*) Toc75 (psToc75) is one of the most abundant proteins in the chloroplast outer envelope membrane (Cline et al., 1981). It associates with precursor proteins in vitro (Perry and Keegstra, 1994; Schnell et al., 1994), and was reconstituted as a cation-selective ion channel in artificial liposomes (Hinnah et al., 1997), suggesting that it forms a major component of the preprotein translocation channel (Bédard and Jarvis, 2005; Kessler and Schnell, 2006; Smith, 2006). Unlike other outer membrane proteins, Toc75 is synthesized as a larger precursor with a bipartite targeting signal (Tranel et al., 1995; Tranel and Keegstra, 1996); the first part is a standard transit peptide for chloroplast import (Inoue et al., 2001) and the second

part acts as an intraorganellar targeting signal that is cleaved by an envelope-bound type I signal peptidase (Inoue and Keegstra, 2003; Inoue et al., 2005; Baldwin and Inoue, 2006).

Arabidopsis (*Arabidopsis thaliana*) possesses four genomic sequences with homology to psToc75 on chromosomes I, III, IV, and V; these are termed *atTOC75-I*, *-III*, *-IV*, and *-V*, respectively (Jackson-Constan and Keegstra, 2001; Eckart et al., 2002). Among them, *atTOC75-I*, *-III*, and *-IV* are highly homologous to one another and to the pea gene, with predicted amino acid sequence identities ranging from 60% to 75%. Previous work demonstrated that *atTOC75-I* is a pseudogene and that *atTOC75-IV* encodes a truncated protein that lacks a transit peptide and is expressed at very low levels (Baldwin et al., 2005). By contrast, atToc75-III is synthesized as a larger precursor with a bipartite transit peptide, like psToc75, and is highly expressed (Inoue and Keegstra, 2003; Baldwin et al., 2005). Disruption of *atTOC75-III* with T-DNA insertions arrested embryo development at a very early stage (the two-cell stage; Baldwin et al., 2005; Hust and Gutensohn, 2006). These results indicate that atToc75-III is the most direct functional ortholog of psToc75.

The fourth Omp85 homolog of Arabidopsis chloroplasts, atToc75-V, is more distantly related to psToc75, sharing only 22% identity (Eckart et al., 2002). A putative pea ortholog of atToc75-V was not associated with the protein translocation machinery, suggesting that its role is not directly related to chloroplast protein import (Eckart et al., 2002). The pea protein appeared to be smaller (apparent size approximately 66 kD) than the conceptual translation of *atTOC75-V* (approximately 80 kD), whereas the latter was predicted to carry a transit peptide. Thus, it was proposed that atToc75-V has an 11-kD targeting sequence that is removed to yield a mature protein of 69 kD (Eckart et al., 2002). However, subsequent work suggested that atToc75-V (a polypeptide of 732 residues, as encoded by the originally annotated open reading frame) was targeted to isolated chloroplasts without undergoing any change in size (Inoue and Potter, 2004). Additionally, the imported protein was similar in size to a native chloroplast protein recognized by an atToc75-V antibody (approximately 80 kD) and was significantly larger than atToc75-III (approximately 75 kD). Based on these observations, and on the absence of evidence supporting a role in protein translocation, the protein was renamed with the more general designation, AtOEP80 (Inoue and Potter, 2004).

The Toc75 and OEP80 subfamilies are both widely distributed in different plant species (Inoue and Potter, 2004). However, in contrast with Toc75, the function of OEP80 remains elusive. Here, we demonstrate that AtOEP80 is essential for viability and reveal that the N-terminal part of the protein (corresponding to the region between the first and second AUG codons of the annotated open reading frame) is not required for its biogenesis or function.

RESULTS AND DISCUSSION

The *AtOEP80* Gene Is Expressed throughout Development

To gain initial insight into the in vivo role of AtOEP80, we examined its mRNA expression using publicly available microarray data and the Genevestigator V3 analysis tool (https://www.genevestigator.ethz.ch; Zimmermann et al., 2004; Grennan, 2006). For comparison, we also analyzed the other expressed Toc75-related Arabidopsis genes (*atTOC75-III* and *atTOC75-IV*), as well as the gene for a major component of the TIC (Translocon at the Inner envelope membrane of Chloroplasts) complex, *atTIC110*. A developmental time course revealed that all four genes are expressed throughout the life cycle (Supplemental Fig. S1A). The *atTOC75-III* and *atTIC110* genes were expressed most strongly, whereas *atTOC75-IV* was expressed at very low levels. The *AtOEP80* gene exhibited an intermediate expression level, equivalent to approximately 25% of that observed for *atTOC75-III*. Interestingly, developmental fluctuations in the expression of *atTOC75-III* and *atTIC110* were paralleled in the *AtOEP80* expression pattern, albeit with reduced amplitude, which is consistent with the hypothesis that the AtOEP80 function is related to plastid biogenesis (Inoue and Potter, 2004).

When expression of the four genes was considered on an anatomical basis (Supplemental Fig. S1B), a similar trend was observed: That is, in most cases, *atTOC75-III* and *atTIC110* displayed the highest levels, *AtOEP80* an intermediate level, and *atTOC75-IV* the lowest level. Interestingly, there were some notable exceptions to this rule, in pollen, mature embryos, and the endosperm. In embryos, *AtOEP80* expression was approximately 40% higher than that of *atTOC75-III*. Given that atToc75-III, like atTic110, is essential during embryogenesis (Baldwin et al., 2005; Inaba et al., 2005; Kovacheva et al., 2005; Hust and Gutensohn, 2006), this observation suggests that AtOEP80 may also be important during seed development.

Inactivation of *AtOEP80* Causes Seed Abortion

To assess the importance of OEP80 in plastids, we identified three different Arabidopsis lines with T-DNA insertions in the *AtOEP80* gene (Fig. 1A). These mutants carry insertions in the tenth intron (*oep80-1*), the fifth intron (*oep80-2*), and the first exon (*oep80-3*) of the gene. With one exception, all T-DNA junction sequences were amplified and sequenced to obtain precise positional information (Fig. 1A); the 3' side of the *oep80-2* T-DNA insertion could not be amplified, presumably because it is incomplete and lacks a left border (LB) or a right border (RB) sequence. Interestingly, analysis of the T-DNA-associated selectable marker in segregating populations of *oep80-1* and *oep80-2* revealed significant deviations from standard Mendelian inheritance: Only two antibiotic-resistant plants were observed for every one antibiotic-sensitive
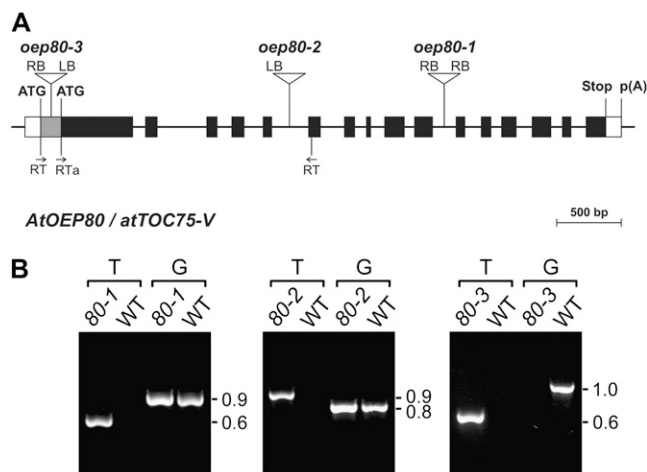
Figure 1. Basic characterization of the *AtOEP80* T-DNA insertion mutants. A, Schematic showing the structure of the *AtOEP80* gene and the location of each T-DNA insertion. Protein-coding exons are represented by black boxes and untranslated regions by white boxes; introns are represented by thin lines between the boxes. The gray area at the 5′ end of exon 1 represents a putative untranslated region, or alternatively encodes a nonessential cleavable peptide. Locations of primers used for RT-PCR analysis (RT; Fig. 4A) are shown. T-DNA insertion sites are indicated precisely, but the insertion sizes are not to scale. ATG, Potential translation initiation codons; Stop, translation termination codon; p(A), polyadenylation site. B, Analysis of mutant genotypes by PCR. Genomic DNA extracted from wild-type and mutant plants (*oep80-1*, *80-1*; *oep80-2*, *80-2*; and *oep80-3*, *80-3*) was analyzed by PCR. Appropriate T-DNA- and *AtOEP80*-gene-specific primers were employed. Two different primer combinations were used: The first (T) comprised one T-DNA primer (RB for *oep80-1*; LB for *oep80-2* and *oep80-3*) and one gene-specific primer (reverse in the case of *oep80-1* and *oep80-3*; forward in the case of *oep80-2*); the second (G) comprised two gene-specific primers flanking the T-DNA insertion site. The results shown for *oep80-1* and *oep80-2* are representative of those obtained for all antibiotic-resistant plants tested; amplification using both T and G indicated the presence of both mutant and wild-type alleles, respectively, and demonstrated that the plants were heterozygous. Results shown for *oep80-3* are representative of those obtained for all homozygotes tested; absence of amplification using the G primers indicated that the wild-type allele was not present. Sizes of the amplicons are indicated at right (in kb).

plant (Supplemental Table S1). These data imply that the homozygous genotype is lethal in each case; they also indicate that both mutants carry just a single T-DNA insertion locus. Consistent with the first conclusion, when we analyzed 78 antibiotic-resistant *oep80-1* plants and 41 antibiotic-resistant *oep80-2* plants, by either progeny testing on selective medium or PCR analysis using gene- and T-DNA-specific primers, all 119 individuals were found to be heterozygous for the mutation. Examples of the PCR-based genotyping experiments we conducted are shown in Figure 1B: PCR reactions (T) utilizing one T-DNA border primer and one *AtOEP80* primer gave a clear amplification product in both mutants, as did additional reactions (G) utilizing two *AtOEP80* gene-specific primers flanking the insertion site.

The absence of homozygous individuals from segregating populations suggested that the mutations might be lethal. To assess the possibility of embryo lethality, we inspected mature siliques of heterozygous *oep80-1* and *oep80-2* plants. In both cases, aborted seeds were observed and these occurred with a frequency of almost exactly 25% (Fig. 2, A and B), strongly supporting the notion that the homozygous genotypes were responsible for seed abortion. Identification of two independent mutant alleles that give rise to the same phenotype is widely accepted as proof of a causal relationship (Sjögren et al., 2004; Baldwin et al., 2005; Puyaubert et al., 2008). Thus, our data provide very strong evidence of an essential role for AtOEP80. Consistent with this conclusion, we observed that the transgenic overexpression of an *AtOEP80* cDNA could efficiently complement the distorted segregation and seed abortion defects of *oep80-1*, enabling the identification of apparently normal homozygous mutants at Mendelian frequency (S.-C. Hsu, R. Patel, P. Jarvis, and K. Inoue, unpublished data).

There are numerous precedents for embryo lethality caused by lesions in chloroplast proteins (Uwer et al., 1998; Apuya et al., 2001). In fact, in a large-scale screen for mutations affecting seed development, >25% of the identified loci were predicted to encode plastidic proteins (McElver et al., 2001). Most relevant among these previous studies are those pertaining to two major components of the chloroplast protein import machinery: atToc75-III (Baldwin et al., 2005; Hust and Gutensohn, 2006) and atTic110 (Inaba et al., 2005; Kovacheva et al., 2005). Interestingly, the aborted seeds in *oep80* plants (Fig. 2A) appeared to be significantly larger than those observed previously in *toc75-III* mutants and were more similar in size to those in the *tic110* mutant (Baldwin et al., 2005; Kovacheva et al., 2005). This suggested that the *oep80* mutation, like *tic110*, may act at a later stage in embryogenesis than *toc75-III*.

Whereas the *toc75-III* mutations appeared to be completely recessive (Baldwin et al., 2005), heterozygous *tic110* plants were visibly pale and exhibited quantifiable defects in chloroplast biogenesis (Kovacheva et al., 2005). In this regard, the *oep80* mutations are more similar to the *toc75-III* mutations, because heterozygotes could not be distinguished from the wild type, not only at a macroscopic level (Fig. 3A), but also in relation to chlorophyll content (Fig. 3B) and photosynthetic performance (Supplemental Table S2). This indicates that a single copy of the *AtOEP80* gene is able to produce sufficient quantities of the protein for normal growth under standard, controlled conditions. The greater dosage dependency of *tic110* may reflect a higher rate of turnover of the atTic110 protein or the absence of excess expression capacity for atTic110 in the wild type.

Homozygous *oep80-1* Embryos Arrest at the Globular Stage

To determine more precisely the stage at which developmental arrest occurs, we conducted a thor-

Figure 2. Embryo lethality of the *oep80-1* and *oep80-2* mutations. A, Appearance of aborted seeds within mature siliques of *oep80-1* heterozygous plants. The aborted seeds are smaller in size than the normal seeds and have a darker, shriveled appearance. B, Frequency of aborted seeds within mature siliques of wild-type, *oep80-1*, and *oep80-2* plants. The data shown are means (±SD) derived from analyses of three or four siliques from each of three to six independent plants per genotype. C, Analysis of embryo development in *oep80-1* using Nomarski optics. Equivalent developmental series for normal (i–iv) and mutant (v–viii) embryos within immature *oep80-1* heterozygous siliques. Normal embryos: i, early globular stage; ii, late globular stage; iii, heart stage; iv, torpedo stage. Corresponding mutant embryos from the same siliques: v, proembryo stage; vi, early globular stage; vii and viii, raspberry-like globular stage. Embryo cell stage names refer to the morphology of the embryo proper. All images are at the same magnification. Bar = 50 μm.
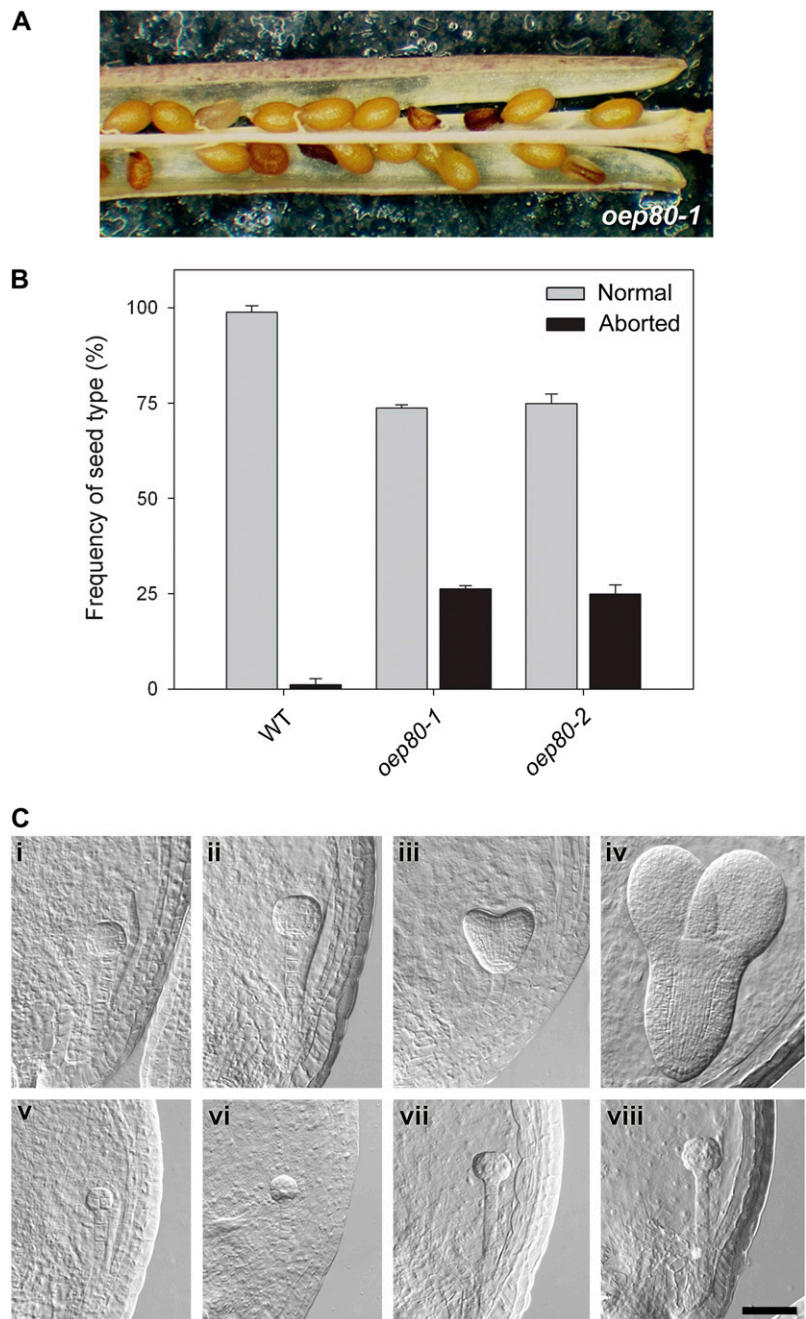
ough examination of developing embryos in wild-type and mutant plants using Nomarski optics. Figure 2C shows equivalent developmental series for normal (i–iv) and mutant (v–viii) embryos within immature siliques of self-pollinated *oep80-1* heterozygotes. When normal embryos were at the globular stage (Fig. 2C, i and ii), mutant embryos (equivalent to 26% of the total number; Table I) were retarded at the proembryo stage (Fig. 2C, v and vi). As normal embryos progressed to the heart stage (Fig. 2C, iii), mutant embryos (equivalent to approximately 24% to 29% of the total number; Table I) developed to the globular stage (Fig. 2C, vii), but began to take on an abnormal, raspberry-like appearance, with protuberances on the surface of the embryo proper (Yadegari et al., 1994; Apuya et al., 2002). By the time the normal embryos had reached the torpedo stage (Fig. 2C, iv), the raspberry-like phenotype of the mutant embryos had become even more pronounced (Fig. 2C, viii). The mutant embryos (equivalent to approximately 22% of the total number; Table I) did not develop beyond the globular stage. In contrast with the situation in *oep80-1* siliques, where two clear, distinct classes of embryos could be observed (normal and mutant), embryos within individual wild-type siliques rarely spanned more than two consecutive developmental stages (Table I).
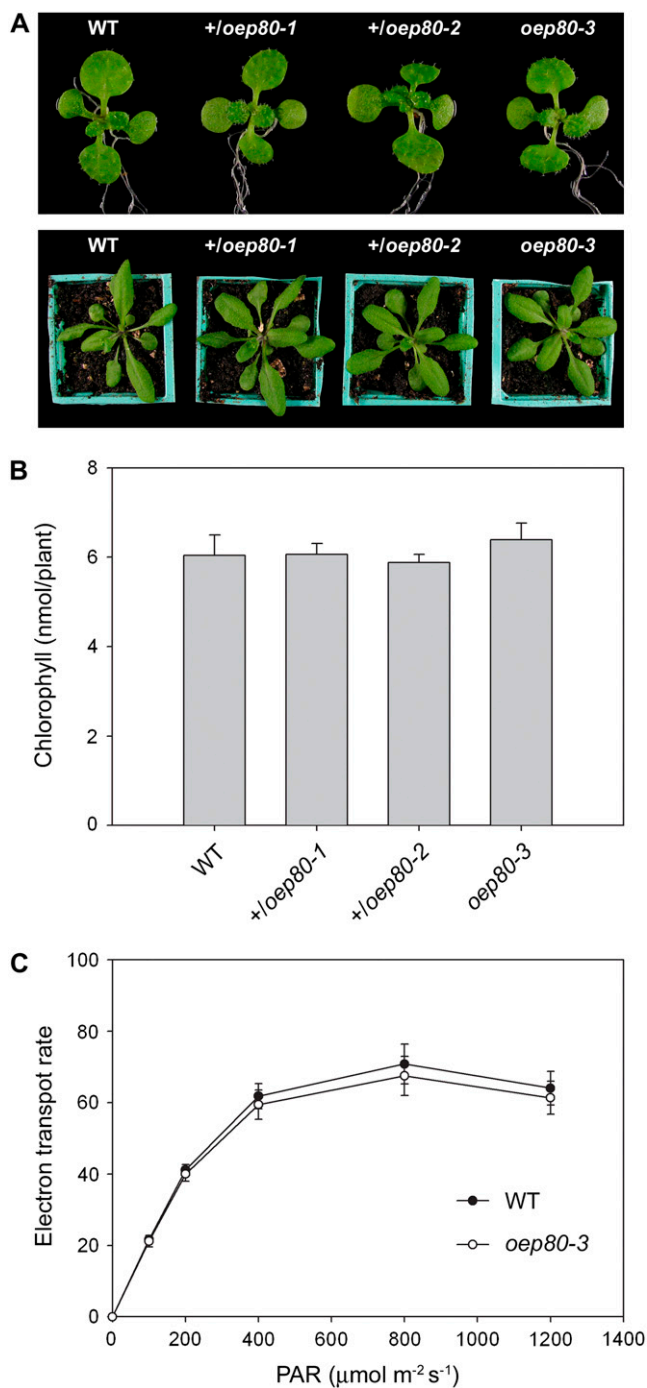
Figure 3. Phenotypic analysis of the *oep80* mutants. A, Plants of the indicated genotypes were grown on selective medium (except for the wild type) in vitro for 8 d, rescued to nonselective medium, and then photographed on day 14 (top). Additional similar plants were transferred to soil on day 14 and then allowed to grow for a further 10-d period prior to photography (bottom). Representative plants are shown in both cases. B, Chlorophyll concentrations in 14-d-old plants grown as described in A were determined photometrically. Values shown are means (±SE) derived from 16 independent samples per genotype, each one containing six plants. Units are nmol chlorophyll *a* + *b* per plant. C, Analysis of photosynthesis in the *oep80-3* mutant. Light response curves of photosynthetic electron transport rates in wild-type and mutant plants were determined by measuring chlorophyll fluorescence.

A very similar raspberry-like, globular-stage arrest phenotype was reported for the atTic110 knockout mutant, *tic110* (Kovacheva et al., 2005). The protuberances on the surface of the embryo proper, responsible for the raspberry-like appearance of the *oep80* and *tic110* mutant embryos, are in fact a characteristic feature of many mutants that arrest during this stage of embryogenesis. It is thought that they are caused by cellular maturation processes that normally occur during late embryogenesis and continue to proceed in the mutants in spite of the block in embryo growth and morphogenesis (Yadegari et al., 1994; Apuya et al., 2002). Unlike *oep80*, the *tic110* mutation was also associated with abnormal, asymmetric, or unsynchronized cell divisions at earlier developmental stages in some embryos (Kovacheva et al., 2005). Because no such early defects were observed in the AtOEP80 knockout, the *oep80* mutant phenotype can be considered somewhat less severe and later acting than *tic110*. Nevertheless, the *oep80*-mediated block in growth occurs considerably earlier than the stage during which photosynthetic establishment normally commences (heart stage; Apuya et al., 2001), and so the data indicate that the role of AtOEP80 is not directly associated with photosynthesis.

The late-acting effect of *oep80* contrasts with the much earlier defect reported for the atToc75-III knockout mutation, *toc75-III* (Baldwin et al., 2005). In *toc75-III*, embryo arrest was observed to occur when the embryo proper was composed of just two cells. Because the two genes are expressed at comparable levels in embryos (Supplemental Fig. S1B), this difference in phenotype severity between *toc75-III* and *oep80* may reflect differing roles of the proteins. Whereas atToc75-III is believed to be the channel responsible for the import of most proteins (Bédard and Jarvis, 2005; Kessler and Schnell, 2006; Smith, 2006), AtOEP80 has been proposed to play a more specialized role in the biogenesis of outer envelope β-barrel proteins, like certain bacterial and mitochondrial Omp85 proteins (Inoue and Potter, 2004).

Homozygous *oep80-3* Plants Are Phenotypically Normal

In contrast with the situation for *oep80-1* and *oep80-2*, the selectable marker associated with the *oep80-3* T-DNA segregated normally, exhibiting standard Mendelian inheritance: three antibiotic-resistant plants were observed for every one antibiotic-sensitive plant (Supplemental Table S1). This implies that the homozygous *oep80-3* genotype is not lethal, which is surprising given the

Values were recorded at different irradiances of photosynthetically active radiation (PAR), ranging from 0 to 1,200 μmol photons m^{-2} s^{-1}. Units for the data shown are μmol electrons m^{-2} s^{-1}, assuming that 84% of the incident light is absorbed and that the transport of each electron utilizes two photons (Meyer et al., 1997; Aronsson et al., 2007). Measurements were done on fully grown leaves from 10 different 29-d-old plants per genotype grown under identical conditions. Values shown are means (±SD).

Table I. *Distribution of embryo phenotypes in single siliques of oep80-1 heterozygotes[a]*

Genotype	Silique[b]	Proembryo[c]	Globular (Raspberry-Like)	Globular	Heart	Torpedo	N.D.[d]	Total Scored	Proportion Delayed or Abnormal
Wild type	4	54	–	–	–	–	9	54	–
	6	1	–	58	–	–	6	59	–
	8	–	–	14	46	–	1	60	–
	10	–	–	1	48	7	0	56	–
	12	–	–	–	9	48	10	57	–
oep80-1	4	54	–	–	–	–	6	54	–
	6	17	–	49	–	–	1	66	0.26
	8	–	17	41	12	–	1	70	0.24
	10	–	16	–	39	1	1	56	0.29
	12	–	14	–	2	47	1	63	0.22

[a]Embryo developmental stage names refer to the morphology of the embryo proper. [b]Siliques were numbered consecutively from the top of the inflorescence, such that the oldest siliques have the highest numbers. [c]Proembryo stage includes one-cell to 16-cell stage embryos. [d]Not determined; seeds that were not classified for technical reasons.

location of the T-DNA in the first exon (Fig. 1A). Families containing only antibiotic-resistant individuals were identified and these were confirmed as *oep80-3* homozygotes by PCR analysis (Fig. 1B). Remarkably, homozygous *oep80-3* mutants were indistinguishable from wild type. The mutant was of a similar size and color to wild type throughout development (Fig. 3A) and contained normal levels of chlorophyll (Fig. 3B). Chlorophyll fluorescence measurements did not reveal any differences in photosynthetic performance between *oep80-3* homozygotes and wild type (Fig. 3C; Supplemental Table S2), nor did assays of nonphotosynthetic development (root length, hypocotyl length in etiolated plants, and de-etiolation efficiency; Supplemental Table S2).

The aforementioned data provide strong evidence that there are no phenotypic consequences associated with the *oep80-3* T-DNA insertion. This initially suggested that the mutant may encode a truncated form of AtOEP80 and that the missing N-terminal region is not essential. To investigate this possibility, we first of all analyzed *AtOEP80* expression by reverse transcription (RT)-PCR. Using the RT pair of amplification primers (which flank the *oep80-3* T-DNA insertion site; Fig. 1A), an amplicon of the expected size was obtained for wild type, but no expression was detected in *oep80-3* (Fig. 4A). However, when the forward amplification primer was replaced with the RTa primer (located downstream of the T-DNA; Fig. 1A), we observed clear evidence of *AtOEP80* mRNA expression in the mutant (Fig. 4A). In fact, the detected transcript was overexpressed in the mutant, relative to wild type, presumably as a consequence of cauliflower mosaic virus 35S enhancer sequences in the T-DNA construct. These data indicate that a truncated *AtOEP80* message is indeed produced in the *oep80-3* mutant.

The N Terminus of "Full-Length" AtOEP80 Is Dispensable

To determine precisely the nature of the *oep80-3* transcript, we amplified its 5′ end by RACE-PCR and se-

quenced the resulting product. The mutant mRNA was found to comprise approximately 86 to 90 nucleotides encoded by the T-DNA LB fused to an *AtOEP80*-encoded sequence at the expected position based on the previously determined T-DNA gene junction sequence (Fig. 1A; Supplemental Fig. S2). This transcript lacks the first AUG codon (AUG1) of the wild-type message and so is predicted to encode a truncated, approximately 74-kD protein of 680 residues starting from the second, in-frame AUG (AUG2); an approximately 80-kD polypeptide of 732 residues is encoded by initiation at AUG1. To test for the presence of this smaller protein, we analyzed isolated chloroplasts from wild-type and *oep80-3* plants by immunoblotting. Surprisingly, the mutant chloroplasts contained an AtOEP80 protein of the same size as that in wild type and this migrated at a position just above atToc75-III (Fig. 4B; see also Supplemental Fig. S3A); the atToc75-III protein has a calculated molecular mass of approximately 75 kD and yet runs significantly faster than the 75-kD standard on a 7.5% SDS-PAGE gel. Assuming that AtOEP80 is approximately 74 kD in size, its slower migration than atToc75-III may be due to posttranslational modification of one of the proteins because there are no obvious differences in amino acid composition.

In an attempt to explain the above data, we used SDS-PAGE and immunoblotting to compare the sizes of different, in vitro-translated AtOEP80 proteins, imported into chloroplasts, with that of the endogenous protein. We previously took a similar approach to show that the full-length protein of 732 residues, following import, migrates in similar fashion to the endogenous protein as recognized by an AtOEP80-specific antibody (Inoue and Potter, 2004). At that time, we had been focusing on determining whether AtOEP80 is synthesized with a cleavable, approximately 11-kD transit peptide, and so might not have detected more subtle mobility differences between the proteins. Here, we used an affinity-purified sample of the antibody (Supplemental Fig. S3B) to improve sensitivity and clarity, and extended the gel electrophoresis time to thoroughly scrutinize any small mobility differences.
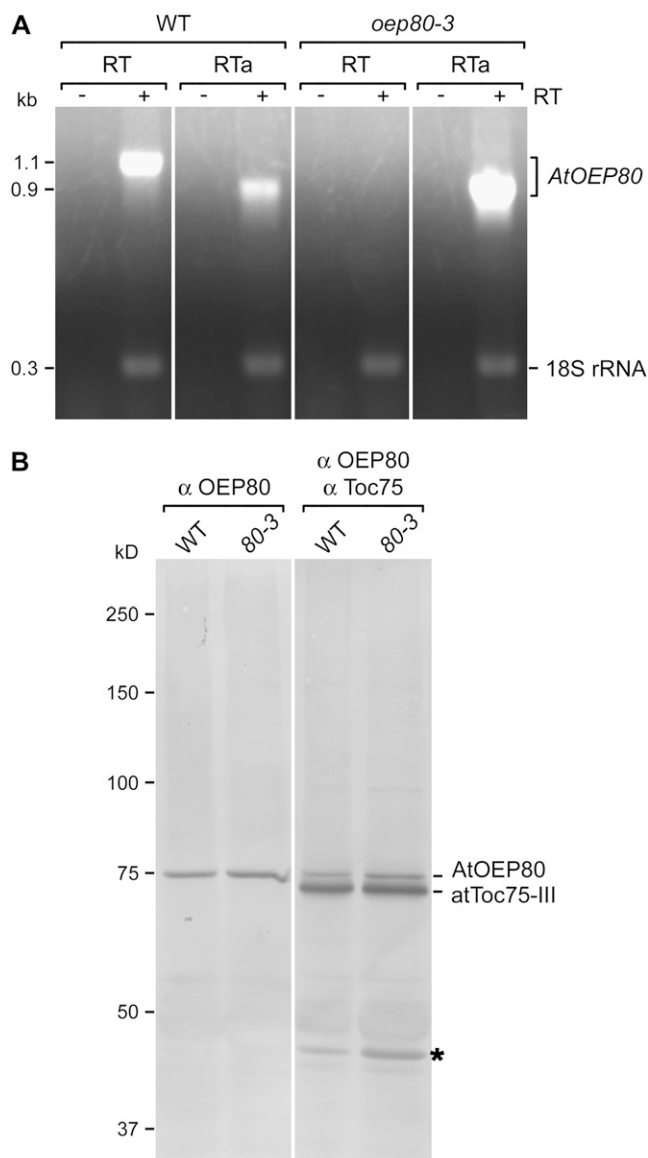
Figure 4. Analyses of mRNA and protein expression in the *oep80-3* mutant. A, Analysis of *AtOEP80* mRNA expression. Total RNA extracted from wild-type and homozygous *oep80-3* mutant plants was analyzed by RT-PCR. Each reaction contained two primer pairs: The first specifically amplified a 1.1-kb fragment from the wild-type *AtOEP80* transcript (locations of the RT primers used are indicated in Fig. 1A) or a 0.9-kb fragment from the wild-type and *oep80-3* mutant transcripts (the forward RT primer was replaced with RTa in this case; see Fig. 1A); the second amplified a 315-bp fragment derived from 18S rRNA and served as a positive control. Reactions lacking reverse transcriptase (−RT) were included as negative controls. Images from different portions of the same gel are separated by vertical lines. Sizes of the amplicons are indicated at left (in kb). B, Analysis of AtOEP80 protein expression. Isolated chloroplast samples (equivalent to 20 μg [left] or 10 μg [right] chlorophyll) were separated by SDS-PAGE and then analyzed by immunoblotting using antiserum against AtOEP80 only (left), or a mixture of antisera against AtOEP80 and psToc75 (right). Protein bands corresponding to AtOEP80 and atToc75-III are indicated at right. Positions of molecular mass standards are indicated at left (sizes in kD); note that the 75-kD standard migrates more slowly than atToc75-III and at approximately the same speed as endogenous

We prepared two translation reactions: one utilizing the full-length *AtOEP80* cDNA as template (AtOEP80 [AUG1]) and another utilizing a truncated cDNA lacking the first 156 nucleotides of the coding sequence and starting from the second AUG codon (AtOEP80 [AUG2]) as template (Fig. 5A, lanes 4 and 10). Whereas the former reaction contained a single, major product of the expected size (approximately 80 kD), the latter contained a number of smaller proteins (presumably corresponding to initiation at downstream AUG codons; predicted sizes 71, 70, 59, 54, and 48 kD) in addition to the expected product of 74 kD. The prominence of alternative initiation products in the second translation reaction most likely reflects the suboptimal context of AUG2 in the translation system used (see Supplemental Appendix S1). In import experiments conducted in vitro, both proteins were recovered in chloroplasts (Fig. 5A, lanes 5 and 11). Proper membrane integration of the 680-residue protein was confirmed in a high-pH wash experiment: The longest translation product was recovered almost exclusively in the membrane fraction following alkaline treatment, whereas the most abundant shorter product was substantially released to the supernatant (Fig. 5B, compare lanes 6 and 7). These data confirm that the first 52 residues of the full-length 732-residue protein are not essential for import or membrane integration. Interestingly, whereas AtOEP80 translated from AUG1 (the 732-residue protein) migrated more slowly than endogenous AtOEP80, that translated from AUG2 (the 680-residue protein) migrated in a very similar position to the endogenous protein (Fig. 5A; compare lanes 5 and 2 and lanes 11 and 8; Fig. 5B, compare lanes 5 and 1 and lanes 7 and 3).

These results may be explained in two different ways. One possibility is that the AtOEP80 protein is normally translated from a noncanonical, downstream initiation codon, even in wild type, with AUG2 being one candidate (see Supplemental Appendix S1; Supplemental Fig. S4). This hypothesis is supported by the fact that the *oep80-3* mutant expresses a protein of the same size as that in wild type (Fig. 4; Supplemental Fig. S3) and by the comigration of the 680-residue protein translated from AUG2 with the endogenous protein in chloroplasts (Fig. 5). It is also noteworthy that the two most similar sequences present in the protein databases (OsI_006101 [EAY84868] and OsJ_005573 [EAZ22090], both from rice [*Oryza sativa*]) align with AtOEP80 only at positions downstream of the second Met. Such noncanonical initiation might have developmental or regulatory significance.

However, in two different in vitro translation systems (wheat germ, Fig. 5A; rabbit reticulocyte, Fig. 5B), initiation at AUG2 appeared to be rather inefficient. Moreover, a recent proteomic study indicated that

AtOEP80. A 40-kD protein band that was nonspecifically recognized by the psToc75 antiserum is indicated with an asterisk. Images from different portions of the same gel are separated by a vertical line.
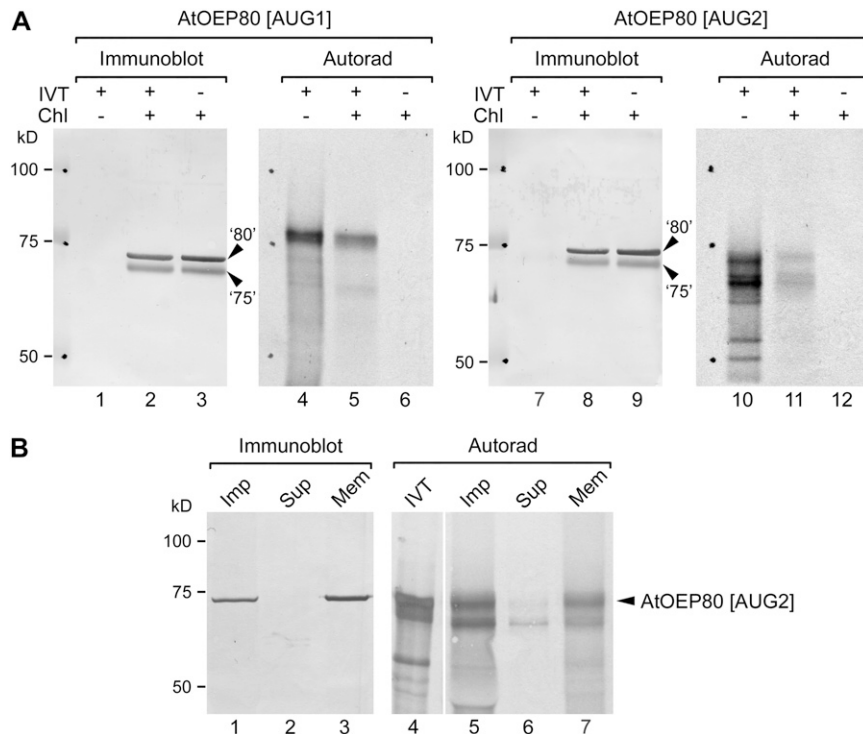
Figure 5. Electrophoretic mobility comparisons between proteins imported into Arabidopsis chloroplasts in vitro and endogenous AtOEP80. A, Radiolabeled long (AtOEP80 [AUG1]; 732 residues) and short (AtOEP80 [AUG2]; 680 residues) forms of the AtOEP80 protein were generated by in vitro translation using different cDNA templates. These were incubated with Arabidopsis chloroplasts under import conditions and then the chloroplasts were recovered. In vitro translation products equivalent to 10% of the amount added to each import assay (IVT+/Chl−), Arabidopsis chloroplasts containing imported, radiolabeled proteins (IVT+/Chl+), and equivalent chloroplast samples lacking imported, radiolabeled protein (IVT−/Chl+) were resolved side-by-side using SDS-PAGE, blotted onto the same membrane, and then analyzed either by probing with AtOEP80 and psToc75 antisera (Immunoblot) or by autoradiography (Autorad). The positions of endogenous AtOEP80 and atToc75-III proteins are indicated at right ('80' and '75', respectively). Positions of molecular mass standards are indicated at left (sizes in kD). Under the conditions used, the endogenous AtOEP80 protein migrated slower than atToc75-III, whereas both proteins ran faster than the 75-kD marker protein. B, In vitro translated, radiolabeled AtOEP80 (AtOEP80 [AUG2]; 680 residues) was incubated with Arabidopsis chloroplasts under import conditions. One-half of the recovered chloroplast sample was subjected to alkaline extraction using 0.1 M Na_2CO_3 and separated into soluble and membrane fractions as described (Inoue and Potter, 2004). In vitro translation products equivalent to 5% of the amount used for the import assay (IVT), unfractionated Arabidopsis chloroplasts containing imported, radiolabeled protein (Imp), and the supernatant (Sup) and membrane (Mem) fractions obtained after alkaline extraction were resolved side-by-side using SDS-PAGE, blotted onto the same membrane, and then analyzed either by probing with AtOEP80 antiserum (Immunoblot) or by autoradiography (Autorad). The position of imported AtOEP80 is indicated at right. Positions of molecular mass standards are indicated at left (sizes in kD); note that the 75-kD marker runs significantly slower than atToc75-III on a 7.5% SDS-PAGE gel.

translation from AUG1 can occur in vivo; of 89 AtOEP80 peptides identified by Dunkley et al. (2006), one (FSSSSIR; positions 10–16 relative to Met-1/AUG1) was found to correspond to the sequence between AUG1 and AUG2 (K. Lilley, personal communication). Thus, an alternative to the noncanonical initiation possibility outlined above is that translation from AUG1 leads to the formation of a 732-residue precursor protein, which is processed to a lower molecular mass form during targeting or membrane insertion. Because the targeting, accumulation, and functionality of AtOEP80 were not detectably altered in the *oep80-3* mutant (Figs. 3 and 4), one may conclude that any cleavable, N-terminal targeting sequence that is present is dispensable. It is noteworthy that neither of the AtOEP80 translation products changed in size upon import (Fig. 5). However, this may simply indicate that proteolytic processing is inefficient in the context of an in vitro protein import assay, as has been observed previously for Tic22 and Toc75 (Kouranov et al., 1999; Inoue and Keegstra, 2003).

CONCLUSION

Our aim was to assess the importance of the plastidic protein, AtOEP80, for plant growth and development. As a first step, we analyzed the expression of *AtOEP80* using publicly available microarray data relative to well-known components of the protein translocation

machinery of the plastid envelope. Expression levels of *AtOEP80* paralleled those of *atTOC75-III* and *atTIC110* throughout development, but at substantially lower levels (approximately 25% of the level of *atTOC75-III*). Interestingly, a different trend was observed in embryos, with *AtOEP80* expression being approximately 40% higher than *atTOC75-III* expression, hinting at an important role for AtOEP80 during embryogenesis. Consistent with this notion, the knockout mutations *oep80-1* and *oep80-2* were embryo lethal in the homozygous state, demonstrating that AtOEP80 plays an essential role during early stages of plastid development. Developmental arrest occurred at a relatively late stage in *oep80* (globular stage embryo proper), which contrasts with the early defect (two-cell stage) caused by loss of atToc75-III (Baldwin et al., 2005). This difference in phenotypic severity may reflect differences in the roles of the proteins: atToc75-III playing a wide-ranging role in the import of many proteins and AtOEP80 a more specialized role, perhaps in the biogenesis of a relatively small subset of proteins. Further experimentation will be required to determine the exact function of AtOEP80. Surprisingly, a third AtOEP80 mutant, *oep80-3*, which carries a T-DNA insertion in the first exon, was found to be viable and indistinguishable from wild type in the homozygous state. In spite of the fact that *oep80-3* expresses a truncated transcript lacking the first AUG codon, the mutant was found to express an AtOEP80 protein of the same size as that in wild type. Together with data from in vitro translation, import, and immunoblotting experiments, this observation led to the conclusion that the N-terminal region of the putative full-length AtOEP80 protein of 732 residues is not required for targeting, membrane insertion, or functionality. This contrasts with the situation for atToc75-III, which requires a bipartite targeting sequence for proper biogenesis (Tranel and Keegstra, 1996; Inoue and Keegstra, 2003). Thus, there are two essential, Omp85-related β-barrel proteins in the outer envelope membrane of chloroplasts, but it would appear that these proteins have quite different requirements for membrane insertion.

MATERIALS AND METHODS

Plant Growth Conditions

All Arabidopsis (*Arabidopsis thaliana*) plants were of the Columbia-0 ecotype. For in vitro growth, seeds were surface sterilized, sown on Murashige and Skoog agar medium in petri plates, cold treated at 4°C, and thereafter kept in a growth chamber, as described previously (Aronsson and Jarvis, 2002). To select for the presence of T-DNA insertions, the following antibiotics were added to the medium: hygromycin B, 15 to 30 μg/mL (*oep80-1*); and sulfadiazine, 11.25 μg/mL (*oep80-2* and *oep80-3*). All plants were grown under a long-day cycle (16 h light, 8 h dark).

Root length measurements were conducted as described previously (Constan et al., 2004), using plants grown on vertically oriented Murashige and Skoog agar plates under standard conditions for 10 d. Hypocotyl length measurements were done using plants germinated on soil and grown in sealed propagators in the dark for 5 d using a published method (Salter et al., 2003). De-etiolation experiments were conducted according to a previous report

(Baldwin et al., 2005) and as described below, using plants grown on Murashige and Skoog medium lacking Suc. Following cold treatment, plates were exposed to standard light for 4 h to promote germination and then kept in darkness for 6 d; then, plates were transferred to continuous light for a further period of 2 d prior to scoring.

Identification of the *oep80* Mutants

The T-DNA insertion lines were obtained from the following sources: *oep80-1* was from the Csaba Koncz laboratory (pool 894, line 89350; Ríos et al., 2002); and *oep80-2* and *oep80-3* were from Genomanalyse im Biologischen System Pflanze-Kölner Arabidopsis T-DNA (GABI-Kat; lines 429H12 and 430F02, respectively; Rosso et al., 2003).

Mutant genotypes were assessed by PCR (Fig. 1B). Genomic DNA was extracted from Arabidopsis plants using a published protocol (Edwards et al., 1991) and PCR was conducted using standard procedures. The primers used were as follows: *oep80-1* forward, 5′-CATGGATTGAAGGAGATGACAAGAG-3′; *oep80-1* reverse, 5′-GAAACGAGCTGGTCCAATGTGTATG-3′; *oep80-1* T-DNA RB, 5′-CAGTCATAGCCGAATAGCCTCTCCA-3′; *oep80-2* forward, 5′-AGTAAG-AACGAAAGATGGTGAGGA-3′; *oep80-2* reverse, 5′-TCACTTTCCCTACACA-GCTTGA-3′; *oep80-2* and *oep80-3* T-DNA LB, 5′-CCCATTTGGACGTGAATGT-AGACAC-3′; *oep80-3* forward, 5′-TCCTTGTTTGTTCATGTGTGTGA-3′; *oep80-3* reverse, 5′-TCCTCACCATCTTTCGTTCTTACT-3′; and *oep80-3* T-DNA RB, 5′-GCAAGTGGATTGATGTGATATCTCCAC-3′. The amplification products were analyzed by agarose gel electrophoresis and stained with ethidium bromide. The location of each T-DNA insertion was determined precisely by the sequencing of PCR products spanning both junctions (except in the case of *oep80-2*, where only one junction was identified).

Chlorophyll Quantification and Photosynthetic Measurements

Chlorophyll was extracted from 14-d-old plants grown in vitro and determined photometrically as described previously (Porra et al., 1989; Aronsson et al., 2003). Photosynthetic electron transport rates (Fig. 3C), as well as the photochemical efficiency of PSII (F_v/F_m) and photosynthetic performance index (Supplemental Table S2), were determined by measuring chlorophyll fluorescence using a continuous excitation fluorimeter (Handy PEA; Hansatech Instruments), according to the manufacturer's instructions and as described previously (Meyer et al., 1997; Strasser et al., 2004). The plants used for these chlorophyll fluorescence assays were grown on selective medium for 8 d (where appropriate), rescued to nonselective medium, and then transferred to soil after 2 weeks.

Isolation of RNA and RT-PCR

Total RNA was isolated from Arabidopsis seedlings with an RNeasy plant mini kit (Qiagen), and used to prepare cDNA with Superscript III and random primers (Invitrogen). Using the resultant cDNA as a template, PCR amplifications were performed using the following *AtOEP80* gene-specific primers (Figs. 1A and 4A): RT forward, 5′-ATGCATTGTCACAACGATGA-3′; RTa forward, 5′-ATGCTCCAGTCGCTAAAGAATC-3′; and RT reverse, 5′-TCT-ACATCCCTCTTCCCTTGAA-3′. Control amplification of a sequence derived from 18S rRNA was performed according to the manufacturer's instructions (Ambion).

Chloroplast Isolation, Import, and Immunoblotting

Isolation of chloroplasts from plate-grown Arabidopsis seedlings and in vitro chloroplast protein import assays were performed essentially as described previously (Fitzpatrick and Keegstra, 2001; Inoue and Potter, 2004). For the preparation of radiolabeled precursor proteins, TNT coupled systems containing wheat germ extract (Fig. 5A) or rabbit reticulocyte lysate (Fig. 5B) were used (Promega). The cDNA construct encoding the short form of the AtOEP80 protein (AtOEP80 [AUG2]; 680 residues) was prepared by subcloning a PCR product (forward primer, 5′-ATGCTCCAGTCGCTAAAGAATC-3′; reverse primer, 5′-CTCGAGTTAGTTCCGCAGACCAAC-3′), amplified using pGEMT-AtOEP80 (Inoue and Potter, 2004) as template, into the pGEM-T Easy vector (Promega). Samples were separated by SDS-PAGE and transferred to a polyvinylidene difluoride membrane (Bio-Rad). Imported proteins were detected by autoradiography. For immunodetection, membranes were incubated with antisera raised against psToc75 or AtOEP80 (see below). Immu-

noreactive proteins were detected using a secondary antibody conjugated with alkaline phosphatase and a 5-bromo-4-chloro-3-indolyl phosphate/nitroblue tetrazolium substrate mixture (Bio-Rad).

A previously described antiserum against residues 325 to 337 of AtOEP80 was employed (Inoue and Potter, 2004). Its specificity was confirmed in a competition experiment, and then the crude serum was purified by affinity chromatography for use in Figures 4 and 5 (Supplemental Fig. S3). Briefly, a 200-μg sample of the antigen peptide (Inoue and Potter, 2004) was coupled to 100 μL of UltraLink iodoacetyl gel (MicroLink peptide coupling kit; Pierce) in the provided minicolumn according to the manufacturer's instructions. The crude serum (300 μL) was applied to the column and incubated at room temperature for 2 h. The unbound fraction was collected, and then the column was washed 15 times with 300 μL of wash buffer (0.7 M NaCl, 0.05% [v/v] Tween 20) and a further three times with 300 μL of phosphate-buffered saline (137 mM NaCl, 2.7 mM KCl, 10 mM Na_2HPO_4, 2 mM KH_2PO_4, pH 7.4). Bound antibodies were eluted with 0.1 M Gly, pH 2.8, immediately neutralized with a 1/20th volume of 1 M Tris-HCl, pH 9, and stored at 4°C until further use.

Embryo Analysis by Light Microscopy

The analysis of cleared wild-type and oep80-1 mutant embryos using Nomarski optics (Fig. 2C) was performed as described previously (Goubet et al., 2003; Baldwin et al., 2005; Kovacheva et al., 2005). A microscope (model BHS; Olympus) equipped for differential interference contrast (model BH2-NIC; Olympus) was employed for these studies.

Sequence data from this article can be found in the GenBank/EMBL data libraries under accession numbers NP_568378, CAB51191, NP_192647, NP_172176, Q43715, EAY84868, and EAZ22090.

Supplemental Data

The following materials are available in the online version of this article.

Supplemental Figure S1. Expression patterns of the *AtOEP80* gene relative to genes for other envelope proteins.

Supplemental Figure S2. Annotated T-DNA LB junction sequence for the oep80-3 mutant, illustrating the structure of the 5′ end of the expressed transcript.

Supplemental Figure S3. Specificity confirmation and affinity purification of the AtOEP80 antibody used in the immunoblotting experiments shown in Figures 4 and 5.

Supplemental Figure S4. In silico analysis of the 5′ region of the *AtOEP80* mRNA.

Supplemental Table S1. Segregation of the T-DNA-associated selectable marker in each of the oep80 mutants.

Supplemental Table S2. Phenotypic analysis of the oep80 mutants, including photosynthetic measurements as well as studies on nonphotosynthetic growth.

Supplemental Appendix S1. Analysis of the 5′ region of the *AtOEP80* mRNA in silico.

ACKNOWLEDGMENTS

LITERATURE CITED

Apuya NR, Yadegari R, Fischer RL, Harada JJ, Goldberg RB (2002) *RASPBERRY3* gene encodes a novel protein important for embryo development. Plant Physiol **129:** 691–705

Apuya NR, Yadegari R, Fischer RL, Harada JJ, Zimmerman JL, Goldberg RB (2001) The Arabidopsis embryo mutant *schlepperless* has a defect in the *chaperonin-60α* gene. Plant Physiol **126:** 717–730

Aronsson H, Boij P, Patel R, Wardle A, Töpel M, Jarvis P (2007) Toc64/OEP64 is not essential for the efficient import of proteins into chloroplasts in *Arabidopsis thaliana*. Plant J **52:** 53–68

Aronsson H, Combe J, Jarvis P (2003) Unusual nucleotide-binding properties of the chloroplast protein import receptor, atToc33. FEBS Lett **544:** 79–85

Aronsson H, Jarvis P (2002) A simple method for isolating import-competent *Arabidopsis* chloroplasts. FEBS Lett **529:** 215–220

Baldwin A, Wardle A, Patel R, Dudley P, Park SK, Twell D, Inoue K, Jarvis P (2005) A molecular-genetic study of the Arabidopsis Toc75 gene family. Plant Physiol **138:** 1–19

Baldwin AJ, Inoue K (2006) The most C-terminal tri-glycine segment within the polyglycine stretch of the pea Toc75 transit peptide plays a critical role for targeting the protein to the chloroplast outer envelope membrane. FEBS J **273:** 1547–1555

Bédard J, Jarvis P (2005) Recognition and envelope translocation of chloroplast preproteins. J Exp Bot **56:** 2287–2320

Bölter B, Soll J, Schulz A, Hinnah S, Wagner R (1998) Origin of a chloroplast protein importer. Proc Natl Acad Sci USA **95:** 15831–15836

Cline K, Andrews J, Mersey B, Newcomb EH, Keegstra K (1981) Separation and characterization of inner and outer envelope membranes of pea chloroplasts. Proc Natl Acad Sci USA **78:** 3595–3599

Constan D, Froehlich JE, Rangarajan S, Keegstra K (2004) A stromal Hsp100 protein is required for normal chloroplast development and function in Arabidopsis. Plant Physiol **136:** 3605–3615

Dunkley TP, Hester S, Shadforth IP, Runions J, Weimar T, Hanton SL, Griffin JL, Bessant C, Brandizzi F, Hawes C, et al (2006) Mapping the Arabidopsis organelle proteome. Proc Natl Acad Sci USA **103:** 6518–6523

Eckart K, Eichacker L, Sohrt K, Schleiff E, Heins L, Soll J (2002) A Toc75-like protein import channel is abundant in chloroplasts. EMBO Rep **3:** 557–562

Edwards K, Johnstone C, Thompson C (1991) A simple and rapid method for the preparation of plant genomic DNA for PCR analysis. Nucleic Acids Res **19:** 1349

Fitzpatrick LM, Keegstra K (2001) A method for isolating a high yield of *Arabidopsis* chloroplasts capable of efficient import of precursor proteins. Plant J **27:** 59–65

Gentle I, Gabriel K, Beech P, Waller R, Lithgow T (2004) The Omp85 family of proteins is essential for outer membrane biogenesis in mitochondria and bacteria. J Cell Biol **164:** 19–24

Gentle IE, Burri L, Lithgow T (2005) Molecular architecture and function of the Omp85 family of proteins. Mol Microbiol **58:** 1216–1225

Goubet F, Misrahi A, Park SK, Zhang Z, Twell D, Dupree P (2003) AtCSLA7, a cellulose synthase-like putative glycosyltransferase, is important for pollen tube growth and embryogenesis in Arabidopsis. Plant Physiol **131:** 547–557

Grennan AK (2006) Genevestigator. Facilitating Web-based gene-expression analysis. Plant Physiol **141:** 1164–1166

Hinnah SC, Hill K, Wagner R, Schlicher T, Soll J (1997) Reconstitution of a chloroplast protein import channel. EMBO J **16:** 7351–7360

Hust B, Gutensohn M (2006) Deletion of core components of the plastid protein import machinery causes differential arrest of embryo development in *Arabidopsis thaliana*. Plant Biol (Stuttg) **8:** 18–30

Inaba T, Alvarez-Huerta M, Li M, Bauer J, Ewers C, Kessler F, Schnell DJ (2005) *Arabidopsis* Tic110 is essential for the assembly and function of the protein import machinery of plastids. Plant Cell **17:** 1482–1496

Inoue K, Baldwin AJ, Shipman RL, Matsui K, Theg SM, Ohme-Takagi M (2005) Complete maturation of the plastid protein translocation channel requires a type I signal peptidase. J Cell Biol **171:** 425–430

Inoue K, Demel R, de Kruijff B, Keegstra K (2001) The N-terminal portion of the preToc75 transit peptide interacts with membrane lipids and inhibits binding and import of precursor proteins into isolated chloroplasts. Eur J Biochem **268:** 4036–4043

Inoue K, Keegstra K (2003) A polyglycine stretch is necessary for proper targeting of the protein translocation channel precursor to the outer envelope membrane of chloroplasts. Plant J **34:** 661–669

Inoue K, Potter D (2004) The chloroplastic protein translocation channel Toc75 and its paralog OEP80 represent two distinct protein families and

are targeted to the chloroplastic outer envelope by different mechanisms. Plant J **39:** 354–365

Jackson-Constan D, Keegstra K (2001) Arabidopsis genes encoding components of the chloroplastic protein import apparatus. Plant Physiol **125:** 1567–1576

Jacob-Dubuisson F, Fernandez R, Coutte L (2004) Protein secretion through autotransporter and two-partner pathways. Biochim Biophys Acta **1694:** 235–257

Kessler F, Schnell DJ (2006) The function and diversity of plastid protein import pathways: a multilane GTPase highway into plastids. Traffic **7:** 248–257

Kouranov A, Wang H, Schnell DJ (1999) Tic22 is targeted to the intermembrane space of chloroplasts by a novel pathway. J Biol Chem **274:** 25181–25186

Kovacheva S, Bédard J, Patel R, Dudley P, Twell D, Ríos G, Koncz C, Jarvis P (2005) In vivo studies on the roles of Tic110, Tic40 and Hsp93 during chloroplast protein import. Plant J **41:** 412–428

Kozjak V, Wiedemann N, Milenkovic D, Lohaus C, Meyer HE, Guiard B, Meisinger C, Pfanner N (2003) An essential role of Sam50 in the protein sorting and assembly machinery of the mitochondrial outer membrane. J Biol Chem **278:** 48520–48523

McElver J, Tzafrir I, Aux G, Rogers R, Ashby C, Smith K, Thomas C, Schetter A, Zhou Q, Cushman MA, et al (2001) Insertional mutagenesis of genes required for seed development in *Arabidopsis thaliana.* Genetics **159:** 1751–1763

Meyer U, Köllner B, Willenbrink J, Krause GHM (1997) Physiological changes on agricultural crops induced by different ambient ozone exposure regimes. I. Effects on photosynthesis and assimilate allocation in spring wheat. New Phytol **136:** 645–652

Paschen SA, Waizenegger T, Stan T, Preuss M, Cyrklaff M, Hell K, Rapaport D, Neupert W (2003) Evolutionary conservation of biogenesis of beta-barrel membrane proteins. Nature **426:** 862–866

Perry SE, Keegstra K (1994) Envelope membrane proteins that interact with chloroplastic precursor proteins. Plant Cell **6:** 93–105

Porra RJ, Thompson WA, Kriedemann PE (1989) Determination of accurate extinction coefficients and simultaneous equations for assaying chlorophylls *a* and *b* extracted with four different solvents: verification of the concentration of chlorophyll standards by atomic absorption spectroscopy. Biochim Biophys Acta **975:** 384–394

Puyaubert J, Denis L, Alban C (2008) Dual targeting of Arabidopsis holocarboxylase synthetase1: a small upstream open reading frame regulates translation initiation and protein targeting. Plant Physiol **146:** 478–491

Reumann S, Davila-Aponte J, Keegstra K (1999) The evolutionary origin of the protein-translocating channel of chloroplastic envelope membranes: identification of a cyanobacterial homolog. Proc Natl Acad Sci USA **96:** 784–789

Reumann S, Inoue K, Keegstra K (2005) Evolution of the general protein import pathway of plastids. Mol Membr Biol **22:** 73–86

Ríos G, Lossow A, Hertel B, Breuer F, Schaefer S, Broich M, Kleinow T,

Jasik J, Winter J, Ferrando A, et al (2002) Rapid identification of *Arabidopsis* insertion mutants by non-radioactive detection of T-DNA tagged genes. Plant J **32:** 243–253

Rosso MG, Li Y, Strizhov N, Reiss B, Dekker K, Weisshaar B (2003) An *Arabidopsis thaliana* T-DNA mutagenized population (GABI-Kat) for flanking sequence tag-based reverse genetics. Plant Mol Biol **53:** 247–259

Salter MG, Franklin KA, Whitelam GC (2003) Gating of the rapid shade-avoidance response by the circadian clock in plants. Nature **426:** 680–683

Schnell DJ, Kessler F, Blobel G (1994) Isolation of components of the chloroplast protein import machinery. Science **266:** 1007–1012

Sjögren LL, MacDonald TM, Sutinen S, Clarke AK (2004) Inactivation of the *clpC1* gene encoding a chloroplast Hsp100 molecular chaperone causes growth retardation, leaf chlorosis, lower photosynthetic activity, and a specific reduction in photosystem content. Plant Physiol **136:** 4114–4126

Smith MD (2006) Protein import into chloroplasts: an ever-evolving story. Can J Bot **84:** 531–542

Stojanovski D, Guiard B, Kozjak-Pavlovic V, Pfanner N, Meisinger C (2007) Alternative function for the mitochondrial SAM complex in biogenesis of {alpha}-helical TOM proteins. J Cell Biol **179:** 881–893

Strasser RJ, Srivastava A, Tsimilli-Michael M (2004) Analysis of the chlorophyll *a* fluorescence transient. *In* G Papageorgiou, Govindjee, eds, Advances in Photosynthesis and Respiration: Chlorophyll Fluorescence, a Signature of Photosynthesis, Vol 19. Kluwer Academic Publishers, Dordrecht, The Netherlands, pp 321–362

Tranel PJ, Froehlich J, Goyal A, Keegstra K (1995) A component of the chloroplastic protein import apparatus is targeted to the outer envelope membrane via a novel pathway. EMBO J **14:** 2436–2446

Tranel PJ, Keegstra K (1996) A novel, bipartite transit peptide targets OEP75 to the outer membrane of the chloroplastic envelope. Plant Cell **8:** 2093–2104

Uwer U, Willmitzer L, Altmann T (1998) Inactivation of a glycyl-tRNA synthetase leads to an arrest in plant embryo development. Plant Cell **10:** 1277–1294

Voulhoux R, Bos MP, Geurtsen J, Mols M, Tommassen J (2003) Role of a highly conserved bacterial protein in outer membrane protein assembly. Science **299:** 262–265

Wu T, Malinverni J, Ruiz N, Kim S, Silhavy TJ, Kahne D (2005) Identification of a multicomponent complex required for outer membrane biogenesis in *Escherichia coli.* Cell **121:** 235–245

Yadegari R, Paiva G, Laux T, Koltunow AM, Apuya N, Zimmerman JL, Fischer RL, Harada JJ, Goldberg RB (1994) Cell differentiation and morphogenesis are uncoupled in *Arabidopsis raspberry* embryos. Plant Cell **6:** 1713–1729

Yen MR, Peabody CR, Partovi SM, Zhai Y, Tseng YH, Saier MH (2002) Protein-translocating outer membrane porins of Gram-negative bacteria. Biochim Biophys Acta **1562:** 6–31

Zimmermann P, Hirsch-Hoffmann M, Hennig L, Gruissem W (2004) GENEVESTIGATOR. Arabidopsis microarray database and analysis toolbox. Plant Physiol **136:** 2621–2632